Cell Prolif. 2001, **34**, 115–134

Pattern of self-organization in tumour systems: complex growth dynamics in a novel brain tumour spheroid model

T. S. Deisboeck*,†,‡, M. E. Berens¶, A. R. Kansal**, S. Torquato††, A. O. Stemmer-Rachamimov†,§ and E. A. Chiocca*,†,‡

**Neurosurgical Service, †MGH-Brain Tumor Center, ‡Molecular Neuro-Oncology Laboratory and §C. S. Kubik Laboratory for Neuropathology, Harvard Medical School, Massachusetts General Hospital East, Charlestown, MA; ¶Neuro-Oncology Laboratory, Barrow Neurological Institute, Phoenix, AZ; **Department of Chemical Engineering, Princeton University, Princeton, NJ, USA; ††Department of Chemistry and Princeton Materials Institute, Princeton University, Princeton, NJ, USA*

Received 6 *June* 2000*; revision accepted* 17 *October* 2000

Abstract. We propose that a highly malignant brain tumour is an opportunistic, *self-organizing and adaptive complex dynamic biosystem* rather than an unorganized cell mass. To test the hypothesis of related key behaviour such as cell proliferation and invasion, we have developed a new *in vitro* assay capable of displaying several of the dynamic features of this multiparameter system in the same experimental setting. This assay investigates the development of multicellular U87MGmEGFR spheroids in a specific extracellular matrix gel over time. The results show that key features such as volumetric growth and cell invasion can be analysed in the same setting over 144 h without continuously supplementing additional nutrition. Moreover, tumour proliferation and invasion are closely correlated and both key features establish a distinct ratio over time to achieve maximum cell velocity and to maintain the system's temporo-spatial expansion dynamics. Single cell invasion follows a chain-like pattern leading to the new concept of a *intrabranch homotype attraction*. Since preliminary studies demonstrate that *heterotype attraction* can specifically direct and accelerate the emerging invasive network, we further introduce the concept of *least resistance, most permission and highest attraction* as an essential principle for tumour invasion. Together, these results support the hypothesis of a self-organizing adaptive biosystem.

INTRODUCTION

In spite of all efforts, the prognosis for patients suffering from highly malignant brain tumours such as glioblastoma (multiforme, termed GBM, WHO grade IV) remains uniformly fatal with a median survival time for patients with GBM of 8 months (Black 1991; Whittle 1996). Pure cytoreductive therapy is ineffective since these tumours have already grossly invaded the surrounding brain parenchyma (Burger *et al.* 1988; Nazarro & Neuwelt 1990; Silbergeld & Chicoine 1997). It has been suggested that not only single cells but entire tumours such as malignant brain

Correspondence: Dr Thomas S. Deisboeck, Molecular Neuro-Oncology Laboratory, Harvard Medical School, MGH-East, CNY-6119, Building 149, 13th Street, Charlestown, MA 02129, USA. Fax: 1 6177265079; E-mail: deisboec@helix.mgh.harvard.edu

© 2001 Blackwell Science Ltd.

tumours may behave as a complex system (Kraus & Wolf 1993; Schwab & Pienta 1996). Here, we investigate this hypothesis further and propose that the tumour as a *complex dynamic and self-organizing system* establishes early on an *adaptive invasive network* as the crucial element in the suggested spatial-temporal progression sequence of proliferation and invasion followed again by proliferation (Suh & Weiss 1984). This would explain why invasive cells left behind after an operation can cause tumour recurrence and thus ultimately fatal outcome. Tumour invasion itself is a complex multistep process involving homotype detachment, enzymatic matrix degeneration, integrin-mediated heterotype adhesion as well as active, directed and random motility (Giese *et al.* 1995; Giese & Westphal 1996). In GBM tumours proliferation, as well as motility, is related to the amplification and rearrangement of the epidermal growth factor receptor (EGFR). As a late step in GBM-progression this genetic event seems to be preceded by a loss of heterozygosity on chromosome 10 (LOH 10), which bears a tumour suppressor gene (Lang *et al.* 1994; Lund-Johansen *et al.* 1992, for reviews see Leon, Zhu & Black 1994 and Louis 1997). Since the EGFR cell surface domain is one of the few known tumour-associated markers and, moreover, since its commonly mutated version, mEGFR, is considered to be tumour specific, several experimental and clinical studies are under way to target these structures in gliomas. Any additional information about the processes in which these receptors are involved is therefore important. Confinement pressure as well as nutrients, toxic components and various polypeptide growth factors establish gradients and the resulting dynamical profiles affect both tumour growth and cell motility. In animal models it is virtually impossible to reproducibly alter and monitor the impact these factors have regionally on the various tumour features. Also, single cell invasion cannot be visualized *in vivo* due to resolution thresholds. In addition, common *in vitro* assays are not well suited to study the interplay of tumour features in the same multidimensional setting. Thus, novel experimental settings have to be developed. At an early stage a GBM tumour can be seen as a large-scale multicellular tumour spheroid (MTS). Without neovascularization growth would eventually plateau in both early stage GBM and MTS. This is caused by the combination of increased mechanical confinement and the onset of central necrosis due to the growth-limiting factor of nutrient diffusion over a r^2-growing surface as compared to a rapidly expanding r^3-volume. Because of the rapid volumetric growth of real GBM tumours, even neovascularization will not be sufficient. Thus both GBM and larger MTS are comprised of large central areas of quiescent, apoptotic and necrotic cells and both also continually shed cells from the surface which in turn can start invasion (Folkman & Hochberg 1973; Hoshino & Wilson 1975; Turner & Weiss 1980; Landry, Freyer & Sutherland 1981; Freyer 1988; Sutherland 1988; Helmlinger *et al.* 1997; Brown & Giaccia 1998).

Using such human glioma spheroids, we have developed a novel *in vitro* model, capable of studying microscopic tumour growth complexity. The strong correlation between proliferation and invasion has implications to large-scale dynamics of early stage GBM tumours. As such the presented findings yield important insights into the growth pattern of tumour systems and support the notion of tumours as *complex dynamic self-organizing biosystems*. Based on these results we then introduce two novel concepts for invasion: the guiding *intrabranch homotype attraction* and the principle of *least resistance, most permission and highest attraction*.

MATERIALS AND METHODS

In vitro model

The human U87MGmEGFR GBM cell line was a kind gift from Dr W. Cavenee (Ludwig Institute for Cancer Research, San Diego, CA, USA). We cultured this cell line in DMEM medium

(GIBCO BRL, Life Technologies™, Grand Island, NY, USA) supplemented with 10% heat inactivated cosmic bovine serum (HyClone®, Logan, UT, USA) and 400 μg/ml G418 (Life Technologies™) in a humidified atmosphere (at 37 °C and 5% CO_2). In addition to the wild-type epidermal growth factor receptor (wtEGFR) these stable-transfected cells coexpress an EGFR variant (mEGFR = ΔEGFR, $EGFR_{vIII}$ (2×10^6/cell)). This specific mEGFR has an in-frame deletion of 801 bp of the coding sequence for the external ligand-binding domain, rendering the receptor constitutively active and incapable of signal-attenuation by down-regulation. This genetic rearrangement is rather common in GBM tumours and confers enhanced tumourigenicity *in vitro* by increasing proliferation and reducing apoptosis (Nishikawa *et al.* 1994). U87MGmEGFR cells have a doubling-time of 20 h and rapidly form MTS in culture after reaching monolayer confluence, which spontaneously detach at a certain size range. We collected the floating U87MGmEGFR MTS with Pasteur-pipettes 2–3 days after changing the medium (pH ≈ 6.4 ± 0.2) and washed them gently in OPTI-MEM® (GIBCO BRL) to eliminate residual serum. The spheroids (≈ 500–700 μm in diameter; $0.7–1.0 \times 10^4$ cells) were then placed in between two layers of growth factor reduced (GFR) matrix, Matrigel® (BIOCAT®, Becton Dickinson, Franklin Lakes, NJ, USA), which forms a reconstituted basement membrane at room temperature. It has been shown that such basement membranes have distinct network structure (Kleinman *et al.* 1986). Initially extracted from the Engelbreth-Holm-Swarm mouse tumour, this specific GFR-matrix variant contains less growth factors (such as EGF, PDGF, TGF-β) as compared to the commonly used Matrigel, however, a similar amount of laminin (61%), collagen IV (30%) and entactin (7%). In order to render the implanted cells more susceptible to nutrient gradients, we then reduced growth factors and extracellular matrix (ECM) proteins further by diluting the gel solution with (serum-free) OPTI-MEM® to a ratio of 3 : 1 GFR-M to medium. The total GFR-M/OPTI-MEM® volume reached 200 μl per well (using a 48-well flat bottom tissue culture treated Multiwell™ plate (FALCON®, Fisher Scientific, Pittsburgh, PA, USA)). Presented are the results of three identical experimental settings, each consisting of 10 wells ($n = 30$). In order to diminish the effects of central MTS quiescence and beginning focal MTS necrosis as well as apoptosis in the invasive branch-tips, the experiments were stopped after 144 h post placement of the MTS. This marked the time point when the pace of volumetric growth becomes non-significant. The one-day increase in volume drops below 15%, which equals less than half the values obtained during the steep growth phase (on average, 33% at 48, 72 and 96 h) and therefore signals the onset of the decelerating phase in this avascular setting. The conditioned medium used as heterotype attractor was harvested from subconfluent U87MGmEGFR monolayer cultures at day 3 (pH ≈ 6.7 ± 0.35).

Histology

Briefly, U87MGmEGFR spheroids were harvested as described above at varying sizes (200–600 μm). Following addition of fibrin and serum the aggregates were fixed in 10% formalin and embedded in paraffin. Blocks were than serially sectioned (thickness = 7 μm) and stained with haematoxylin and eosin. In order to assess the proliferative activity staining with the cell cycle-unspecific MIB-1 monoclonal antibody (Amac Inc., Westbrook, ME, USA; 1 : 75 dilution) was performed. The MIB-1 antibody detects the nuclear Ki-67 antigen, which is expressed throughout the cell cycle so that only quiescent (G_0) cells remain unstained. For quantitative evaluation of this Ki-67 reactivity an online image analysis-system (Image-Pro® Plus; Media Cybernetics L.P., Silver Spring, MD, USA) connected to an Olympus® BX60 light-microscope was used. Central sections were analysed, whereby the Ki-67 proliferation index represents the percentage of the total MTS area, A_{MTS} (see below) occupied by MIB-1 positive cells.

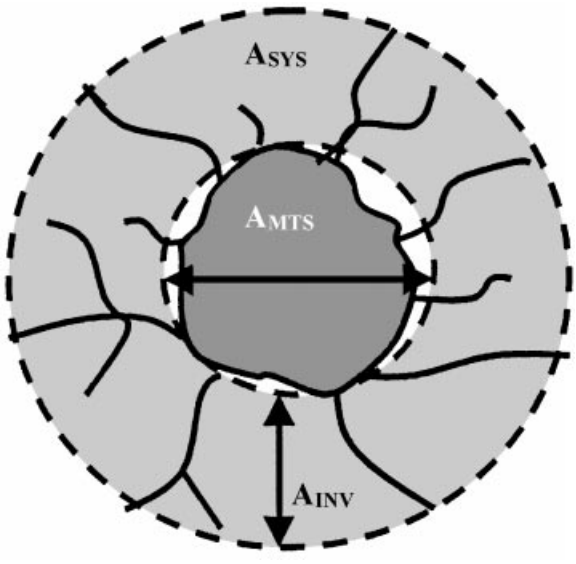


Figure 1. Schematic of the tumour system. The dark grey region is the real MTS, which is approximated as the small broken circle (of diameter D_{MTS} and area A_{MTS}). The large broken circle approximates the extent of the entire system (with area A_{SYS}). The region between the two circles (shown light grey) denotes the invasive area (with A_{INV}). Compare with Figure 3A.

Image analysis and calculations

A Nikon inverted light microscope connected to an online image analysis system was used for morphometric analysis. Changes were recorded daily. The maximum orthogonal diameters of the MTS were measured (original magnification: × 40) and the average, D_{MTS}, was used to calculate the volume, V_{MTS}, of the MTS core and its surface area, S_{MTS}, assuming it to be a sphere.

$$V_{MTS} = \frac{\pi D_{MTS}^3}{6} \tag{1}$$

$$S_{MTS} = \pi D_{MTS}^2 \tag{2}$$

In addition, a cross-sectional area of the core, A_{MTS}, was obtained using D_{MTS} and assuming a circular cross-section (see Fig. 1).

$$A_{MTS} = \pi\left(\frac{D_{MTS}}{2}\right)^2 \tag{3}$$

Similarly, D_{SYS} was measured using the average of orthogonal diameters of the invasive chains and from this A_{SYS} calculated, assuming circularity. Finally, the area of the invasive region alone, A_{INV}, was calculated from:

$$A_{INV} = A_{SYS} - A_{MTS} \tag{4}$$

The invasive velocity, V_{INV}, was determined by calculating change in the difference between the MTS radius, R_{MTS}, and the tumour system radius, R_{SYS}, between a time t *and* $t + \Delta t$.

$$V_{INV} = \left(\frac{(R_{SYS}(t+\Delta t) - R_{MTS}(t+\Delta t)) - (R_{SYS}(t) - R_{MTS}(t))}{\Delta t}\right) \tag{5}$$

Note that this equation assumes that the volumetric growth of the MTS pushes the invasive cells away, rather than overtaking and incorporating them. The values thus reflect a measurement for the invasive edge-motility. (Note also that at t_0, $R_{SYS} = R_{MTS} \rightarrow V_{INV} = 0$ μm/24 h). We propose that in order to characterize the dynamic strength of the entire growing biosystem the growth of the invasive region must be related to that of the spheroid. The reason for this assumption is that invasion has to start from the proliferative (rim) fraction of the implanted spheroid and therefore should be linked in its dynamics. Because invasion in this sandwich-system is predominantly two-dimensional (between the ECM layers), the cross-sectional area of the spheroid, A_{MTS}, was compared to the invasive area, A_{INV}, as a function of time, t.

$$\frac{A_{INV}(t)}{A_{MTS}(t)} = f(t) \tag{6}$$

If no feedback between invasion and proliferation is present at the time scales of the experiment, $f(t)$ would be expected to be directly proportional to t. As such, this linear dependence on time can be factored out of the expression leading to the form

$$\frac{A_{INV}(t)}{A_{MTS}(t)} = \frac{\tau(t)}{\kappa} \cdot t \tag{7}$$

in which $\tau(t)$ represents the dynamic strength and κ is a parameter discussed below. In this form, a constant value of τ is expected for a system with no feedback between invasion and proliferation. Any time dependence within τ then indicates some feedback between the two processes. More specifically, if (as we hypothesize) the tumour behaves in a self-organizing fashion, fluctuations in τ away from a constant value should be corrected for through a feedback mechanism. This process predicts a specific form for $\tau(t)$ of dampened oscillations in time, i.e.

$$\tau(t) = \tau_0 \exp(-at)\cos(\varpi t + \phi), \tag{8}$$

in which τ_0 is a dimensionless constant equal to the long time value of τ, a is a dampening constant with units t^{-1}, ω is a frequency and ϕ is a phase shift. If such a form for τ could be observed, it would support the hypothesis of tumours as self-organizing systems. Rearranging equation 7, the dynamic strength of the biosystem, $\tau(t)$, can be expressed in terms of readily measurable experimental variables as

$$\tau(t) = \kappa\left(\frac{A_{INV}(t)/A_{MTS}(t)}{t}\right) \tag{9}$$

Since the MTS size does not decrease (see Results) it is evident that τ only increases if the system expands rapidly (through invasion) over the continually increasing (total) observation period, t. This 'strength' is thus largely dependent on the tumour's intrinsic capacities but also related to the environmental conditions. As such the factor κ is an uncharacterized time-independent parameter, which depends on the specific environment being invaded. To express its impact on the overall dynamics, this factor has units of time. However, lacking specific microstructural analysis data of the gel, κ is currently kept constant (= 1 [hours]) for all experiments reported in here, including the attractor experiment.

The values given below are the mean values for 30 wells (± SEM). For statistical analysis, the Mann–Whitney rank sum test was used to compare step-wise changes between two sequential time points. In addition, for the invasion velocity, v_{INV}, we applied the Kruskal–Wallis test followed by the Student-Newman-Keuls method for all pairwise comparisons. For both tests, a P-value of < 0.05 was considered to be statistically significant.

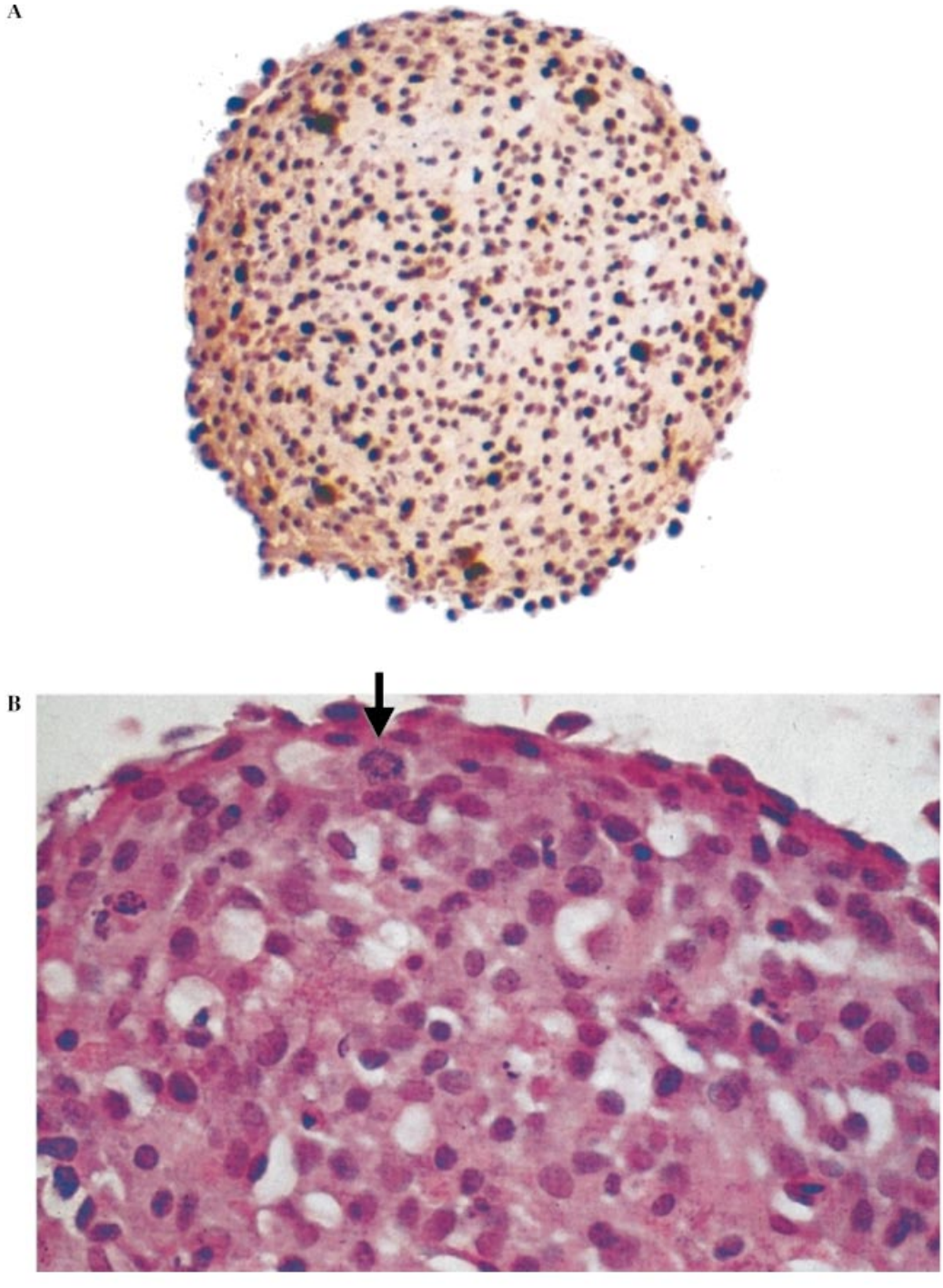


Figure 2. (A) MTS histology. MIB-1 staining of a central section (original magnification × 100). Note the dense layering of positive, i.e. dark brown cells at the MTS surface (MTS diameter = 450 μm). **(B) MTS histology.** H & E staining of a central section (original magnification × 400). Note the lucid areas and apoptotic nuclei in the centre as well as mitotic figures (arrow) in the proliferative rim.

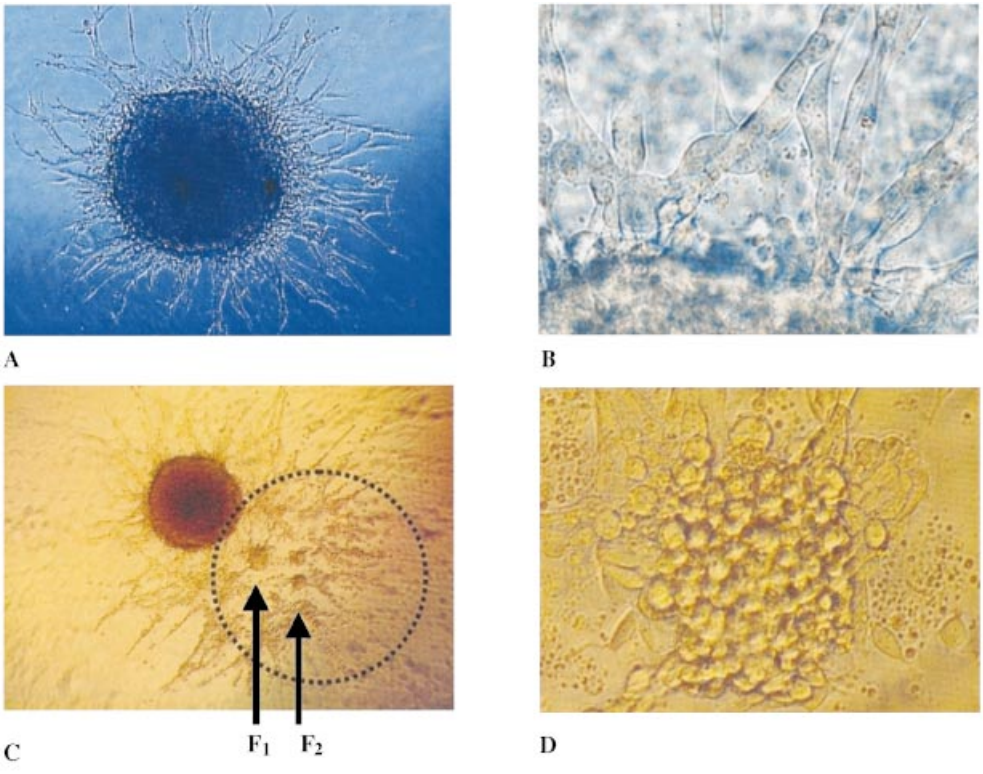


Figure 3. (A) MTS assay. Note invasion pathways centrifugal evolving from the central (darkened) MTS at 24 h (original magnification × 100). **(B) MTS assay.** Note single cell composition of the invasive branches (original magnification × 400). **(C) MTS assay** with attractor site (10 µl conditioned medium). Note asymmetrical invasion area with elongated pathways and cluster structures towards the attractor site (symbolized by dotted line) at 120 h (original magnification × 40). Note different sized cluster structures, whereby F_1 and F_2 corresponds to their spatio-temporal origin. See text for details. **(D) MTS assay.** Multicellular (F_1) cluster (original magnification × 400). See Figure 3C for details.

RESULTS

Histology

The MIB-1 staining reveals an inverse relationship between MTS size and proliferative index: for example, by increasing from 180 µm to 310 µm and 460 µm in diameter the Ki-67 index declined from 34% to 25% and 23%, respectively. The proliferative cells (Fig. 2A) tend to be more densely arranged in the surface layers of the MTS. In the centre of the larger MTS cells are less dense with separate lucid areas and apoptotic nuclei are occasionally noted. In the larger spheroids (> 450 µm) the superficial cells (2–3 layers) are orientated so that their long axis is parallel to the circumference of the spheroid forming a thin fascicle (Fig. 2B; arrow points to a mitotic figure). On the other hand cells in the centre of the MTS are haphazardly orientated, with no particular relationship to each other or to the surface of the MTS.

MTS dynamics

After being placed into the sandwich assay, the MTS grows and shed cells rapidly start to spread into the surrounding ECM-gel (Fig. 3A). These specific invasive patterns consist of advancing

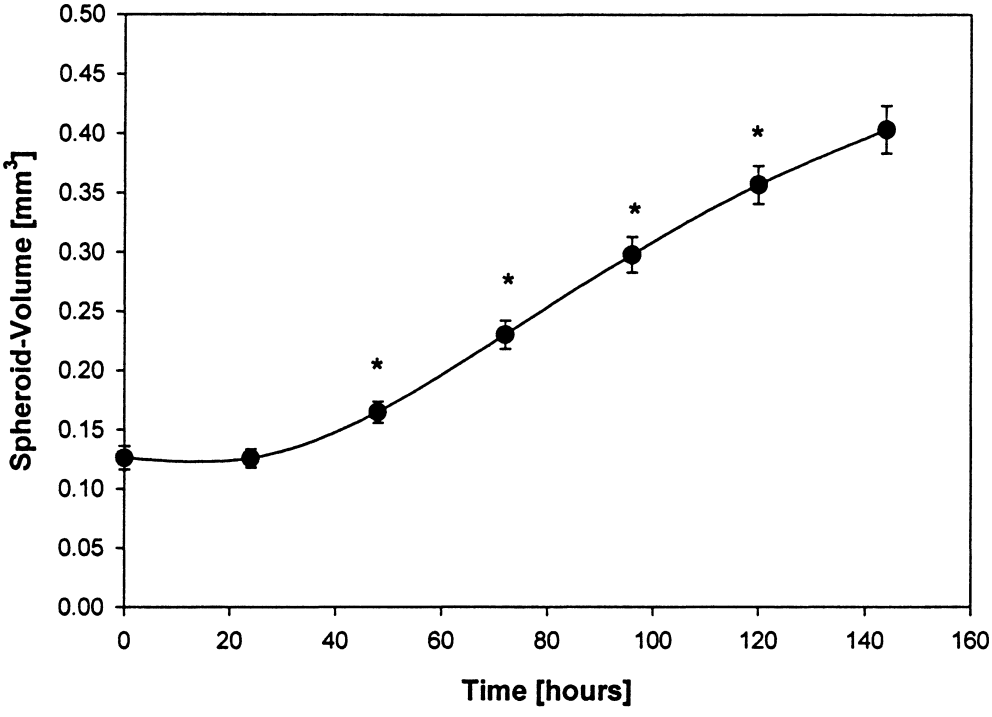


Figure 4. Volumetric growth vs. time ($n = 30$; ± SEM; $^*P < 0.05$).

chain-like single cell branches with increasing branch width towards the proliferative core (Fig. 3B).

As described in Fig. 4, the volumetric growth, V_{MTS}, follows decelerating kinetics with an early lag phase, followed by a steep growth period and finally a decelerating growth phase. Consequently, MTS growth can be mathematically described by both the Gompertz function and the logistic function whereas the rarely used Bertalanffy equation gives less accurate results (data not shown). See Marusic *et al.* (1994) for a review of the mathematical models describing MTS growth.

During the same period the invasion area, A_{INV}, increases significantly as well (Fig. 5). Curve-fitting and measurement of the correlation coefficient show that invasion and volume are strongly correlated (correlation coefficient = 0.996; FitStdErr = 0.00042). Consequently, especially at higher volumes the 95% confidence interval for the volume-invasion curve is small and predictions appear precise.

The specific sandwich assay setting allows primarily for a two-dimensional invasive spread. To be able to compare both features, we express the MTS growth two-dimensionally by using only the 2D-expansion of the central MTS slice (A_{MTS}). The ratio of invasion area to MTS area increases steadily with a maximum (total) increase between 72 and 96 h (data not shown). The increase over 24 h ([24-h]-net-gain) of invasion area and MTS area is depicted in Fig. 6. It emphasizes the steep onset of invasion at 24 h whereas the MTS growth ceases after placement into the gel. During the next 24 h, the MTS area starts to expand and the invasion area continues to increase with the same gain as before. Over the remaining observation period, both gain per time step with maximum values for the expanding MTS area at 72 h vs. 96 h for the invasive area. The ratio of the percentage values ($INV_{[\%]}/MTS_{[\%]}$ = arabic number on the top of the columns)

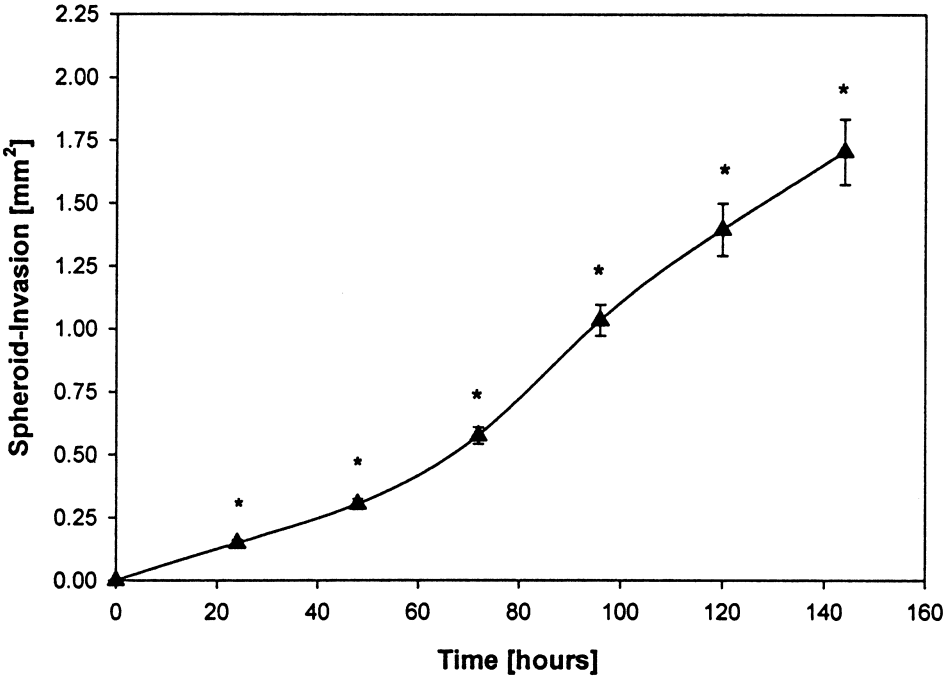


Figure 5. Invasion vs. time ($n = 30$; ± SEM; $^*P < 0.05$).

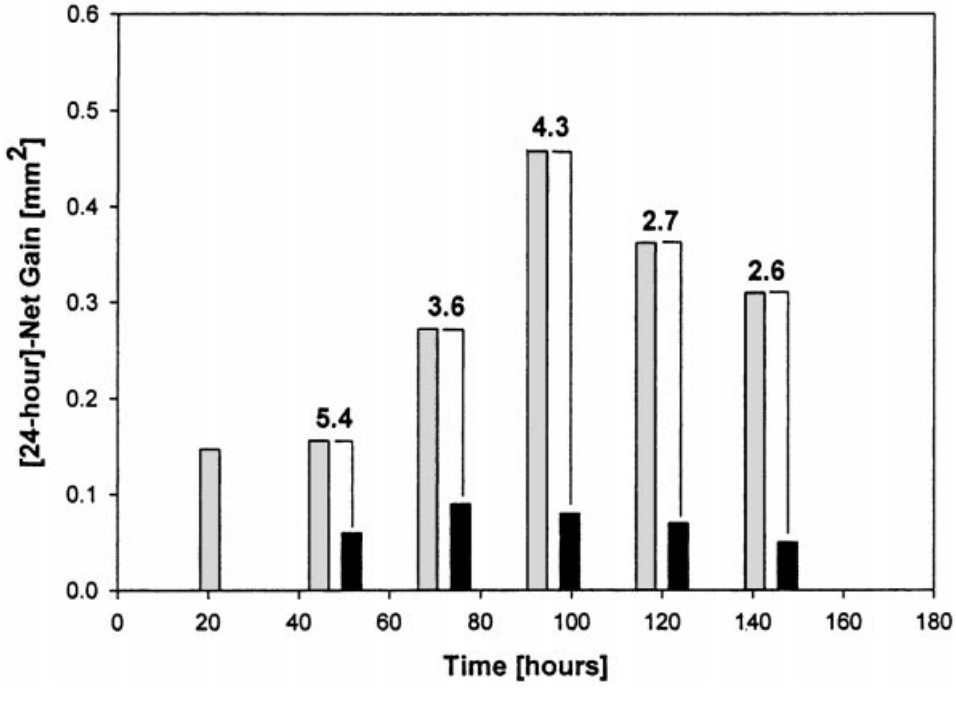


Figure 6. [24-h]-net gain for MTS area (■) and invasion area (▒). The top numbers indicate the percentage net gain-ratio ([INV/MTS]) for each time-step.

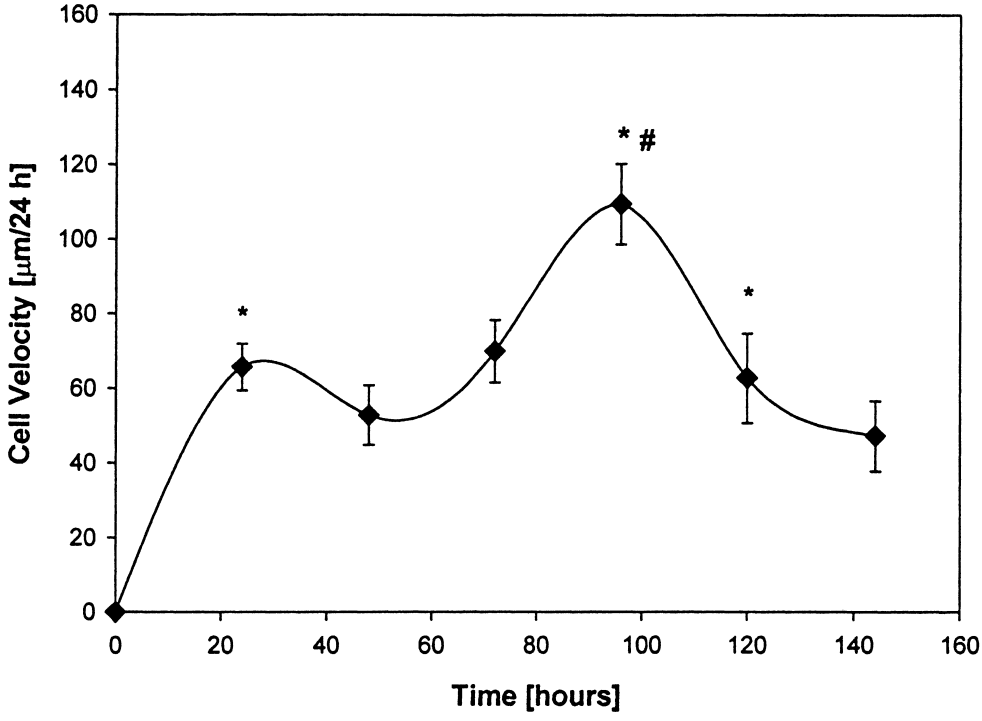


Figure 7. Cell velocity profile vs. time ($n = 30$; ± SEM; $*P < 0.05$; $\#P < 0.05$ (Student–Newman–Keuls method for pairwise multiple comparison procedures)).

shows two peaks, at 48 and at 96 h, respectively. The declining values at 120 and 144 h represent the decelerating growth phase of an established biosystem.

The model also shows a steep increase in invasive (edge) cell velocity, V_{INV}, measured per 24 h (Fig. 7). Depicted is the average value of V_{INV} on opposite sides of the system with a significant increase (*) at 24 h and a significant peak of 109 μm/24 h (*#) at 96 h (followed by a significant decrease (*)), corresponding to the second peak of the net-gain ratios (compare with Fig. 6).

The dynamic strength, τ, has a mean value of 0.0187 (SEM: 0.00048; $\kappa = 1$ h) (Fig. 8) and reveals a three phase behaviour. Whereas, phase I is characterized by the aforementioned steep invasion increase followed by an increasing MTS growth, which led to the first peak in the percentage values of the [24-h]-net-gain, phase III is determined by a general decrease of the system's dynamic strength (see also Fig. 6). This is likely due to the limited nutrition and a potentially slightly diminished fluid phase of the gel, which in turn can lead to an increase in mechanical confinement. Phase II, however, shows a steep increase between 72 and 96 h, with a minimum and maximum at approximately 60 and 100 h, respectively. The maximum equals the peak of the invasive edge velocity and marks the onset of phase III. The MTS volume at 60 h for the minimum τ (0.0177) is approximately 0.198 mm^3. This time point falls within the period during which volume starts to increase significantly (see also Fig. 4) and corresponds to the increasing [24-h] gain of the invasion area after 48 h (see also Fig. 6). Therefore, the MTS volume at the minimum τ seems to be a threshold value for the system's dynamics and consequently is termed 'critical'. The corresponding invasive area for this time-point is approximately 0.429 mm^2.

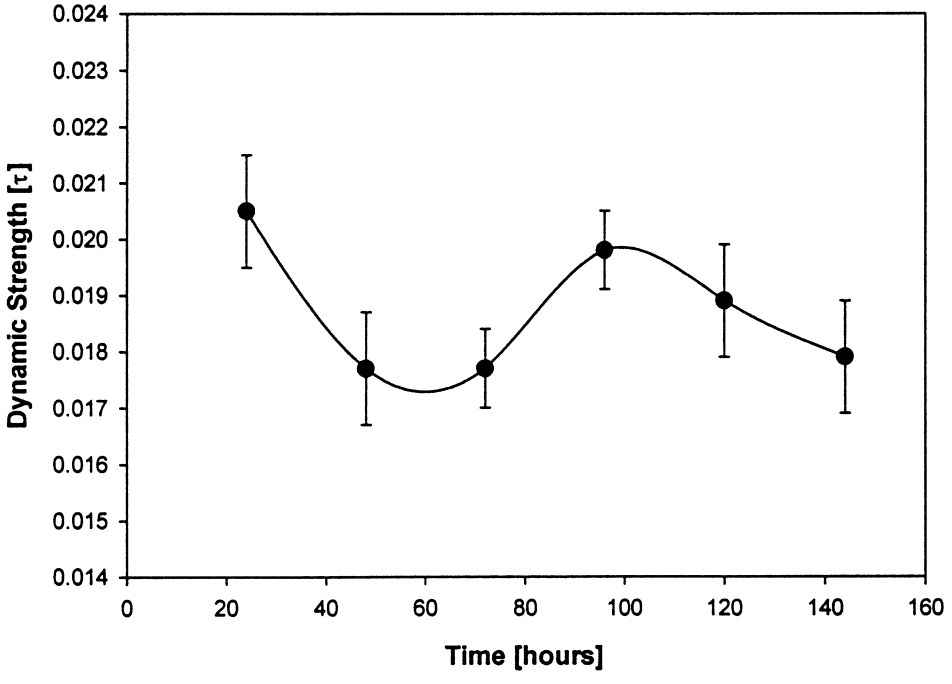


Figure 8. Dynamic strength vs. time ($n = 30$; ± SEM; $k = 1$ h).

MTS dynamics with 'heterotype attractor'

To demonstrate the adaptive capacity of the challenged tumour system using our microtumour model, we now describe the impact of 10 µl conditioned medium (CM) as a (pseudo)heterotype attractor. We added the CM at $t = 0$ h into the right side of the ECM-gel (for schematic, see dotted circle in Fig. 3C). The intention was to locally reduce the gel resistance (by raising the fluid content) and to regionally increase the nutrient concentration for the advancing tumour cells (along a yet undetermined diffusion gradient). Although this impact should result in changes in κ (see equation 9), κ is still kept at 1 [hours] (as in the standard MTS-assay) lacking more specific microstructural analysis data of the gel.

Again, over 144 h MTS growth follows decelerating growth dynamics, with a seized, even slightly shrinking MTS volume over the first 48 h. The difference in volumetric growth at 144 h between the assays with and without the additional attractor (0.318 mm^3 and 0.403 mm^3, respectively) is relatively moderate (Table 1).

However, the averaged invasion area at 144 h of almost 6 mm^2 is more than three times larger than the 1.7 mm^2 in the standard MTS-assay without additional attractor. Moreover, the maximal radial extension of the invasion area towards the attractor side is more than doubled compared to the opposite control area (1390 µm compared to 583 µm) in this experiment. Thus, the invasive network develops predominantly towards the attractor site and specific multicellular aggregates (F_1 and F_2-clusters (see Fig. 3C,D) emerge between 96 and 120 h. These clusters are not static in size. While the MTS grows and the invasive network further advances, F_2-clusters derive spatial-temporally after F_1 and continually gain size (F_2: $V = 0.0017$ mm^3 at 168 h) parallel to a decreasing, however, still much larger F_1. Note also, that the clusters are located within the attractor region suggesting the guiding influence of a heterogeneously diffusing single attractor site on

Table 1 MTS assay with attractor site. MTS-volume, invasion and dynamic strength vs. time

Time [h]	MTS-Vol. [mm^3]	MTS-Invasion [mm^2]	MTS-τ
0	0.087	0	/
24	0.080	0.227	0.042
48	0.082	1.233	0.112
72	0.129	2.862	0.128
96	0.188	4.547	0.119
120	0.255	5.515	0.094
144	0.318	5.970	0.073

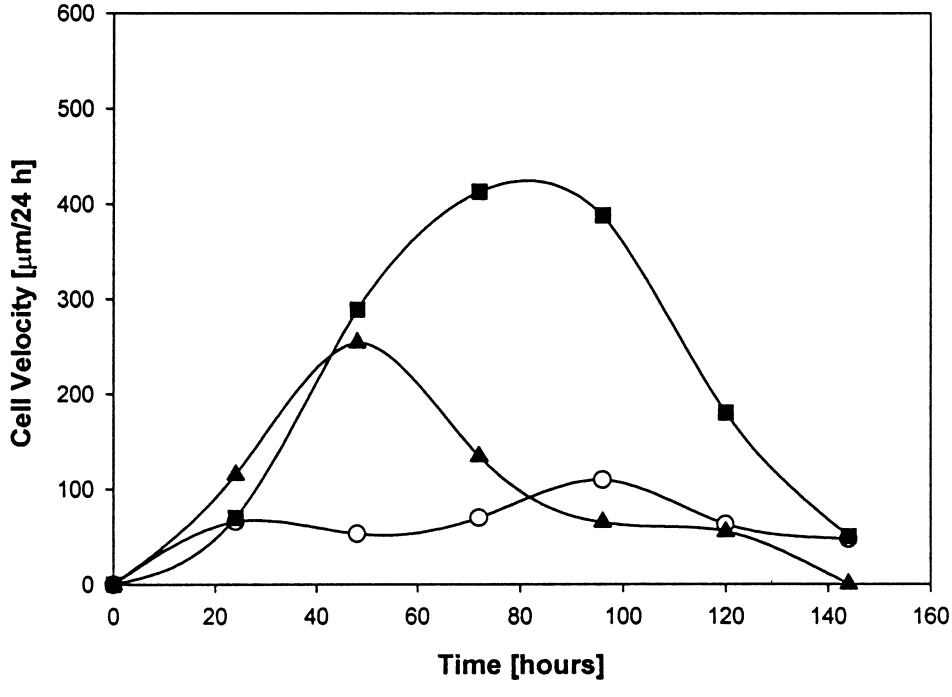


Figure 9. Cell velocity profile of attractor experiment vs. standard MTS assay vs. time. The dynamics on the side towards the attractor substance (conditioned medium) are represented by ■, the opposite side (control) are represented by ▲ and the standard MTS assay are represented by ○.

structural pattern, emerging elements and overall invasiveness. The distance between the MTS and the cell aggregates is also dynamically changing and increases with $V_a = 90$ μm/24 h (MTS $\Leftrightarrow F_1$) and $V_b = 29$ μm/24 h ($F_1 \Leftrightarrow F_2$), respectively (measured between time 120 and 144 h as well as 144 and 168 h, respectively).

The average invasive edge velocity, V_{INV}, on the attractor side is 231 μm/24 h compared to the velocity on the opposite side of only 110 μm/24 h. The peak velocity for each sides are reached at 48 and 72 h (attractor side) corresponding to earlier stages in the exponential volumetric growth phase than the peak velocity in the standard MTS-assay (at 96 h). The increased invasive velocity also persists longer on the attractor side, with the difference between attractor and control sides reaching a maximum at 96 h (Fig. 9). Again, this is the time at which clusters

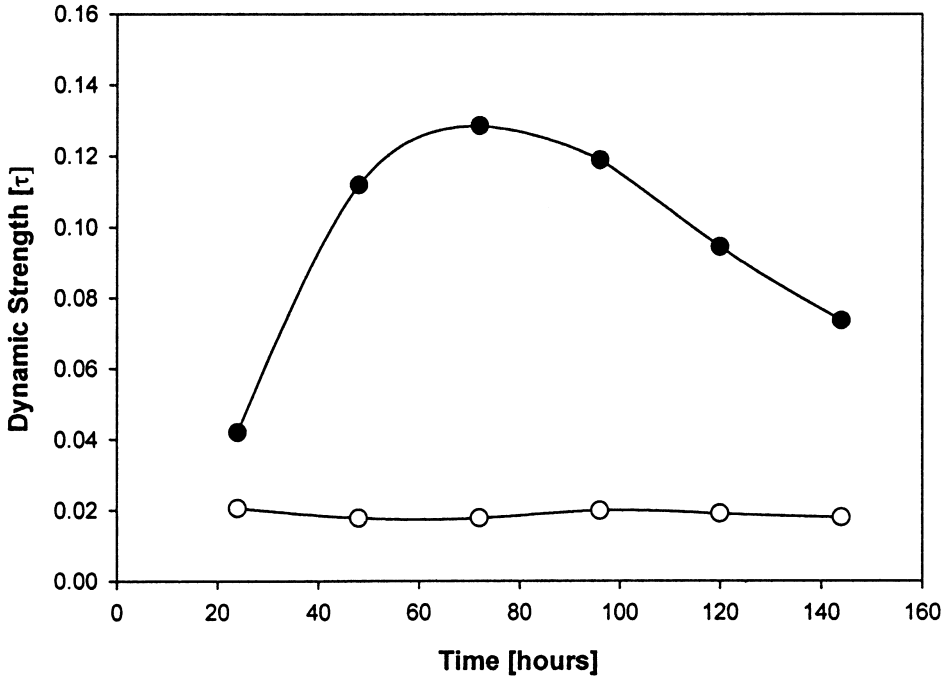


Figure 10. Dynamic strength of attractor experiment (●) vs. standard MTS assay (○).

begin to develop. The peak velocity at the attractor side is over 400 μm/24 h, which is almost four times higher than the peak velocity in the standard MTS-assay at 96 h. Thus, in this experiment the nonreplenished attractor source does not only guide but seemingly also accelerate the system towards its site.

The dynamic strength, τ, shows an immediate and very steep increase without indications of a precise 'critical' volume (Fig. 10). This rapid increase is caused by an early 5.4-fold increase in invasion area at 48 h followed by a delayed 1.5-fold rise in volume (72 h). After a maximum at 72 h the curve declines rapidly, reaching almost starting values of 0.07 (Mean: 0.095 (SEM: 0.0132)). At 72 h, the peak τ of 0.128 is 6.4-times higher and reached 24 h earlier than the peak τ in the standard MTS-assays without additional attractor. Despite the initial increase in invasion, the maximum (total) 24-h gain for both invasion and MTS area is again reached at 96 h. The initial diameter of the spheroid used in the attractor experiment (D_{MTS} = 550 μm) is within the range for the ones used in the standard MTS-assay. Consequently, the difference of τ between the two groups at 24 h is predominantly caused by the rapid onset of invasion between t = 0 h and 24 h in the attractor experiment.

DISCUSSION

In order to investigate the systemic development of a microscopic tumour over time and to study multidimensional key features such as proliferation and invasion in the same setting we have developed a novel sandwich assay by placing multicellular human GBM spheroids in between

two layers of growth factor reduced matrigel. Like many other glioma and nonglioma cell lines these U87MGmEGFR MTS cells rapidly form spheroids in confluent monolayer cultures. We harvested the MTS once they detached and floated in the medium. This is not just considerably faster compared to the spinner-flask method or the liquid overlay technique (Sutherland, McCredie & Inch 1971; Carlsson 1977; Yuhas *et al.* 1977), but also largely avoids asymmetries in the surface, which would otherwise affect the regional onset of invasion. However, the MTS size range chosen in our setting does not allow conclusions about the early growth phase (100–300 μm). Since our MTS derive from one focus of the monolayer, the resulting spheroid should be composed of a more homogenous, potentially monoclonal cell population than the heterogeneous aggregates obtained with other techniques. Using the specific reconstituted basic membrane gel the MTS cells grow in a nonreplenished environment thus mainly depend on the initial supplemented nutrition and their own autocrine/paracrine growth promoting and growth inhibiting factors. In comparison, Tamaki *et al.* (1997) studied invasion of C6 rat glioma cells into a collagen type I based assay for over 12 days, whereby the medium superlayer had to be changed every 3 days. This necessarily alters the conditions during the phase between 48 and 96 h, which we have found to be very important from a kinetic standpoint. The same authors also report about a second set of experiments with a 5-day observation period without changing the medium superlayer. We argue that any such superlayer may compromise the spatio-temporal nutrient, toxicity, growth factor and growth inhibitor profiles and thus impact the dynamics of the tumour system. Experimental assays such as ours, which are capable to properly model the relation of two key features are rather rare. For example, common (2D) migration assays use focal density as a trigger to start single cell motility (Giese *et al.* 1996). If the migration rate of particular cancer cell lines exceeds the proliferation rate, the central trigger rapidly loses its effectiveness, limiting the experimental time frame in these settings. Conversely, when the proliferation rate exceeds motility, active migration can barely be distinguished from passive mechanical pushing. Other assays such as cell proliferation- and invasiveness assays (Repesh 1989; Parish, Jakobsen & Coombe 1992) as well as agarose gels for MTS growth evaluation focus on only one single tumour feature and represent mostly endpoint measurements, with little capability to study the complex dynamics of the multifeatured system.

In our assay, volumetric growth follows the principle of decelerating Gompertzian-like growth dynamics. Tumour invasion and volumetric growth are closely correlated. To study the proliferation-invasion relationship over time we have developed a term, called τ, which represents the *dynamic strength* of the expanding biosystem, depending not just on intrinsic factors but also on extrinsic (environmental) permission, κ. After placing the spheroid in between the layers the initial raise in τ is caused by the marked increase of invasion at 24 h with a concomitant significant increase in invasive edge velocity. Nonetheless, this substantial invasion alone cannot sustain the positive dynamics and in fact, both, invasion increase and velocity cease at this level. Only after further volumetric growth is induced (between 24 and 48 h) and a specific threshold is exceeded (between 48 and 72 h), invasion appears to be triggered and continues to increase rapidly at a higher level. After an invasion dominated first maximum, the net-gain (percentage) ratio of both key features shows a second maximum simultaneously (at 96 h), at the very same time when invasive edge velocity and dynamic strength reach peak values as well. We therefore argue that the increase of τ after the minimum inflexion point at 60 h represents the influence of a surpassed *critical* MTS volume, which induces and maintains the invasion needed to increase the overall dynamics by expansion. Invasion, which has to start topographically as shed cells from the proliferating MTS surface should then also be functionally linked to the corresponding volumetric growth rate of the MTS. This is supported by our observations that volume and invasion are closely correlated and that both [24-h]-net-gain curves correspond very well after 48 h. However, it has

to be stated that if volumetric growth would only push invasion passively the maximum for both gains should be reached simultaneously and not as in our assay separated by 24 h. Therefore our results indicate a more complicated regulatory process behind tissue invasion than mechanic pressure by the tumour core. The maximum of the dynamic strength curve after 100 h represents the end of the steep increase of systemic extension. We hypothesize that this maximum represents another specific volume, which harbors a critical central quiescence/necrosis fraction due to an insufficient nutritive supply and catabolic exchange as argued by Folkman & Hochberg (1973), mounting central toxicity (Freyer 1988) or external mechanical confinement. In fact, such solid stress inhibits the growth of multicellular tumour spheroids and Helmlinger *et al.* (1997) determined a threshold at 45–120 mmHg in agarose. Since the volume of the tumour grows as r^3, its surface area however, only as r^2, normal extension of the MTS surface is accompanied by an even more sustained increase in volume (even if the cell packaging density increases). The solid tumour would have to increase its surface area even more in order to facilitate nutritive supply and would have to aim to reduce the consistency of the adjacent material, which would otherwise restrain further growth and inevitably lead to the onset of central necrosis. One such option (without raising the mechanical confinement pressure even further) is a systemic surface area extension through single cell invasion. If this hypothesis holds true however, we would expect a specific tumour volume to be linked to the onset of invasion, related to a specific external pressure and the tumours' interstitial pressure (and other parameters *in vivo* such as neovascularization). According to this assumption, the correlation of invasion with the tumour volume should remain precise, even at larger tumour volumes (i.e. at 'later' tumour stages). Our curve-fitting results (data not shown) reveal exactly this relation even at the MTS level. An advantage for using volume, as opposed to surface, is that it can incorporate yet unconsidered features such as quiescence and necrosis. We therefore believe we have found strong evidence for the existence of such a critical volume for the onset of invasion in our experimental system. If this containment evading mechanism exists, we have to further postulate that the inductive mechanical pressure determining the critical volume and the onset of invasion, respectively, is lower than the solid stress-inhibition threshold defined in the agarose assays. In other words, invasion should be triggered before the volume-plateau is reached, which is exactly what we see. Thus, we see the result of 2 'critical' volumes: the first lower one, i.e. the original implanted MTS at time 0, which triggers the rapid onset of invasion at time 24 h by virtually shedding all newly generated cells after the first doubling-time. This in turn induces volumetric growth (48 h) followed by another increase in invasive gain at 72 h. Thus tumour volume and invasion seemingly induce each other, further supporting the aforementioned concept, that the onset of invasion should facilitate further volumetric growth. Consequently, one has to postulate also a 'critical' extent of invasion capable of triggering the proliferative MTS rim to 'follow'. The second, upper critical MTS volume is determined by the lack of nutrition and signals, as suggested by Folkman & Hochberg (1973), the need for neovascularization in an *in vivo* setting. Chignola *et al.* (1999) reported oscillating growth pattern for 9 L and U118 glioma MTS on agar, but did not investigate the relationship of these proliferative oscillations to invasion. Our results indicate that in a tumour system proliferative and invasive key-features interact and that therefore the dynamics of the entire system are not dependent on one single feature only. Moreover, a maximum ratio of both parameters can be achieved simultaneously, which may in fact be required in order to gain maximum velocity of cell invasion. The observed behaviour of τ is consistent with *dampened oscillations*. While only one period is visible in the time frame accessible here, this lends additional credence to the proposition that invasion and proliferation in fact control one another. For these reason and for the fact, that τ fluctuates within a relatively small range of 0.0028 (Median: 0.0187) we argue, that the system shows signs of *self-organization*.

The peak invasive cell velocity of 109 μm/24 h in our assay is in good agreement with the 4.8 μm/hour Chicoine & Silbergeld (1995) reported for single invading C6 cells *in vivo*. At 96 h, the peak velocity corresponds to a maximum volumetric increase and therefore reflects the concept of cell density driven single cell motility proven in 2D-migration assays. Most interestingly, the invasive tumour cells seem to follow each other along a cell density-gradient forming *chain-like* pattern, previously only shown for neural precursor cells (Lois, Garcia-Verdugo & Alvarez-Buylla 1996). To our knowledge, these single cell invasive branching patterns have not been described before for cultured gliomas, presumably due to the distinct experimental settings chosen by other investigators. For example, referring to the results of Nygaard *et al.* (1995), who found normal rat brain cells can in fact invade the spheroids, we argue that in this rodent model more pronounced xenogeneic effects may influence the underlying mechanisms, which in turn should have a distinct effect on the evolving structural patterns. Nonetheless, our results correspond well with their finding of a substantial reduction of brain aggregate volume between 48 and 96 h, indicating a steep invasion during this period. We propose an *intrabranch homotype attraction* of tumour cells causing the specific observed patterns. According to this concept, cells would follow each other because of increasing autocrine stimuli and paracrine attraction, e.g. transforming growth factor-alpha (Ekstrand *et al.* 1991), hepatocyte growth factor/scatter factor (Koochekpour *et al.* 1997) or extracellular matrix proteins (Enam, Rosenblum & Edvardsen 1998) and lesser mechanical resistance in a preformed path. Given an ongoing discharge of cells from the proliferative MTS rim, such a mechanism would inevitably lead to a continuous *imprinting* of pathways (termed *oncological plasticity*) and a delayed increase of velocity within the established paths to maintain the networks carrying capacity. This is further supported by our finding, that the highest invasive edge velocity is not measured at the beginning, when the [%]-increase of the invasive area is the highest, but later, when the system established itself. It seems likely that besides the required MTS volume increase, a sufficient invasive network has to be in place in order to advance cells within the network more efficiently and therefore the entire system more rapidly. Besides the concept we presented above to explain why invasion can likely trigger proliferation, we add now that homotype attraction within the emerging network induces the proliferative MTS rim to discharge more cells into the net, i.e. triggering the aforementioned volumetric growth. This leads to the picture of a *self-sustaining* tumour system. The fact that invasion continues to increase significantly at 144 h even though the volumetric growth becomes nonsignificant may argue for the establishment of a (temporary) self-sustaining invasive system *per se*, which becomes less trigger-dependent and only delayed down-regulated.

In agreement with the literature the quantitative immunohistochemistry revealed an inverse relationship between the MTS size and its proliferative activity (Sutherland, McCredie & Inch 1971). As Haji-Karim & Carlsson (1978), who found no occurrence of central necrosis in human U118 glioma spheroids below a diameter of 700 μm, we were unable to detect an expanding central necrotic area within our spheroid size range. However, several sparse necrotic foci and apoptotic cells could be found preferentially in the centre of larger spheroids, indicating the nearing onset of central necrosis. We attribute the differences in cell orientation between the surface layers and the centre of the MTS to the impact of the increasing mechanical pressure gradient (towards the centre). Wakimoto *et al.* (1996) documented the predictive significance of Ki-67 labelling indices in high-grade gliomas. Thus, extrapolated to the macroscopic setting, the linkage of proliferation and invasion has also prognostic implications: if invasion is correlated with the proliferative indices in the tumour rim, their prognostic value may in fact in part derive precisely from that coupling, which emphasizes the role of invasion for outcome. Finally, these conclusions are further supported by our preliminary findings that larger spheroids (> 750 μm) indeed show relatively less invasion (data not shown).

Most interestingly, by adding a defined volume of conditioned medium as a *(pseudo-)heterotype attractor* the kinetics of the evolving network are substantially altered as demonstrated through the shift in peak invasion velocity (for both sides) to the left of the volume curve. This result and the finding that invasion is much more influenced than volumetric growth supports the notion that a strong attractor can evoke invasion, seemingly uncoupled of tumour growth. This is of substantial interest since the standard MTS experiments, as stated above, revealed a strong correlation of volumetric growth and invasion. The behaviour of τ demonstrates its sensitivity to invasion changes: despite this distinct impact, however, and although the attractor influences the dynamics on the opposite (control) side as well, a steeply increasing τ returns at the end of the observation period to almost initial values. As in the standard MTS-assay, limited nutrition and raising confinement (due to a gradual drying of the gel) presumably add to the declining dynamics. But the delayed onset of volumetric growth further indicates that increased invasion to a certain extent may trigger volumetric growth, which (over time (i.e. an increase in t)) can cause τ to rebound. These findings strongly support our hypothesis of a *complex, regionally responsive and globally adaptive biosystem*, suggesting an interplay of related features, which to a certain extent can temporarily be influenced separately if the external impact is strong enough. Nonetheless, if invasion here in fact triggers volumetric growth the increase is kept within limits and an overshooting response (if compared to the volume of the standard MTS-assay at 144 h) is clearly prevented, suggesting a sufficient regulatory mechanism. The finding, that the maximum net gain in invasion area and MTS area is again reached at time 96 h as in the standard assays supports this notion further. This leads to the novel concept of *least resistance, most permission and highest attraction* as an essential principle guiding malignant tumour invasion. It adds attraction to the least resistance concept proposed and investigated earlier by Eaves in 1973. In fact, Bernstein, Goldberg & Laws (1989) as well as Pedersen *et al.* (1993) found that xenografted human glioma cells migrate along myelinated fibres, which represent least resistance paths as studied by oedema spread (Geer & Grossman 1997).

We also found that specific structural elements, *multicellular clusters*, can emerge towards the attractor site. Our analysis shows that, unlike in the experiments of Friedl *et al.* (1995), the clusters in our assay derive from ad hoc aggregating single tumour cells within the invasive net at a later stage and not from cell nodules earlier assembled in the MTS shell. The ability of single invading cells to eventually form clusters has been described earlier by Straeuli, (Straeuli, In-Albon & Haemmerli 1983) who implanted rabbit V2 carcinoma cells in an *in vivo* model. Bernstein *et al.* (1991) discussed the possibility that on site division may contribute to C6 clustering in matrigel and in preliminary studies we indeed found MIB-1 positive cells within the clusters (data not shown). Tamaki *et al.* (1997) stated that the Ki-67 labelling indices in the boundary zone are lower than for the entire invasive area, again suggesting proliferative cell subpopulations within the invasive area. Their C6 spheroid cultures showed small clusters at day 5, which corresponds very well with the emergence of cluster structures in our assay between day 4 and 5. This is important in order to address the concern that our structures may represent retraction foci of invasive cells aggregating within a deteriorating environment. Since aggregates develop in both models at the end of the steep increase of invasion, it appears that the emergence of clusters signals the onset of a conservative phase in the expansion of the biosystem. However, our results also indicate that once formed, these clusters are nonstatic in size and location, which indicates that they may obey turnover with active cell input- and output-fractions. Since the distance to the tumour core increases three times faster than the distance between both cluster populations, it seems that the cell throughput-rate at the F_1 cluster is considerably higher than at the F_2. This in turn would support the notion of a *hierarchically guided system* with a decreasing invasive velocity towards the higher confinement in the boundary zone (close to the plastic wall). However

we cannot exclude the possibility that the intrinsic mechanical pressure generated by the MTS pushes both cluster populations outward, especially since the percentage increase in volume exceeds the one in invasive area for the period of interest (120 vs. 144 h). Referring to their emergence at the former crossover points of invasive branches, we hypothesize that these clusters originally emerge at attractor sites (i.e. nutritive sources and/or low resistance spots) and that these aggregates may have guiding influence on invasive dynamics in a *nonlinear* matter.

Clearly, one must not overstate the results obtained from a single cell line, much less from a single presented attractor experiment. More experiments are currently under way in our laboratory to evaluate the impact of distinct growth promoting and inhibitory factors as well as variations in mechanical confinement pressure on the emerging invasive network. However, if the underlying microstructure of the ECM-gel indeed affects the invasive pattern as it for example should influence the diffusion gradient of the attractor substances it will be challenging to reproduce similar initial conditions. Much will depend on the success to characterize κ in order to be able to compare systems in different experimental setting. This strongly suggests the need of both the concomitant microstructural analysis of the gel (with methods such as Synchrotron-analysis or microtomography) as well as the computational analysis of the resulting invasive pattern.

CONCLUSION

We have developed a novel *in vitro* microtumour model allowing the online analysis of proliferation and invasion with the option of controlled regional impact. In here proliferation and invasion are strongly correlated and both rely on each other for the dynamical expansion of the entire system in a heterogeneous environment. Thus the presented findings provide more evidence that tumours are indeed *complex dynamic biosystems*. We also proposed two novel concepts for invasion: the guiding *intrabranch homotype attraction* principle and the principle of *least resistance, most permission and highest attraction*. Both concepts now need to be investigated in more detail using experimental *in vitro* and *in vivo* settings in combination with computational modelling. By no means can the presented *in vitro* model claim completeness. Nonetheless, by improving this model continually more important insights into the fascinating complex dynamics of these adaptive biosystems may be expected. Since invasive tumour cells are widely thought to be responsible for both, diffuse-disruptive infiltration and tumour recurrence and thus ultimately for treatment failure the understanding of these mechanisms is essential in order to develop novel and more successful targeting strategies against this yet fatal disease.

ACKNOWLEDGEMENT

This work was supported in part by grants CA84509 and CA69246 from the National Institutes of Health as well as by the Carolyn Halloran Fellowship for Brain Tumor Research to T.S.D. and a Guggenheim Fellowship to S.T. The authors like to thank Drs Jerome B. Posner (Memorial Sloan-Kettering Cancer Center), James P. Freyer (Los Alamos National Laboratory) and Hans-Juergen Reulen (University of Munich) for inspiring discussions and Dr David N. Louis (Harvard Medical School) for critical review of the manuscript. The authors acknowledge Ms. Andrea Cutone and Ms. Sarah Jhung for valuable technical assistance.

REFERENCES

Bernstein JJ, Goldberg WJ, Laws ER JR (1989) Human malignant astrocytoma xenografts migrate in rat brain: a model for central nervous system cancer research. *J. Neurosci. Res*. **22**, 134.

Bernstein JJ, Laws ER JR, Levine KV, Wood LR, Tadvalkar G, Goldberg WJ (1991) C6 glioma-astrocytoma cell and fetal astrocyte migration into artificial basement membrane: a permissive substrate for neural tumors but not fetal astrocytes. *Neurosurg*. **28**, 652.

Black PM (1991) Brain tumors. *N. Engl. J. Med*. **324**, 1555.

Brown JM, Giaccia AJ (1998) The unique physiology of solid tumors: opportunities (and problems) for cancer therapy. *Cancer Res*. **58**, 1408.

Burger PC, Heinz ER, Shibata T, Kleihues P (1988) Topographic anatomy and CT correlations in the untreated glioblastoma multiforme. *J. Neurosurg*. **68**, 698.

Carlsson J (1977) A proliferation gradient in three-dimensional colonies of cultured human glioma cells. *Int. J. Cancer* **20**, 129.

Chicoine MR, Silbergeld DL (1995) Assessment of brain tumor cell motility in vivo and in vitro. *J. Neurosurg*. **82**, 615.

Chignola R, Schenetti A, Chiesa E *et al.* (1999) Oscillating growth patterns of multicellular tumour spheroids. *Cell Prolif*. **32**, 39.

Eaves G (1973) The invasive growth of malignant tumours as a purely mechanical process. *J. Pathol*. **109**, 233.

Ekstrand AJ, James CD, Cavenee WK, Seliger B, Pettersson RF, Collins VP (1991) Genes for epidermal growth factor receptor, transforming growth factor α, and epidermal growth factor and their expression in human gliomas in vivo. *Cancer Res*. **51**, 2164.

Enam SA, Rosenblum ML, Edvardsen K (1998) Role of extracellular matrix in tumor invasion: migration of glioma cells along fibronectin-positive mesenchymal cell processes. *Neurosurg*. **42**, 599.

Folkman J, Hochberg M (1973) Self-regulation of growth in three dimensions. *J. Exp. Med*. **138**, 745.

Freyer JP (1988) Role of necrosis in regulating the growth saturation of multicellular spheroids. *Cancer Res*. **48**, 2432.

Friedl P, Noble PB, Walton PA *et al.* (1995) Migration of coordinated cell clusters in mesenchymal and epithelial cancer explants in vitro. *Cancer Res*. **55**, 4557.

Geer CP, Grossman SA (1997) Interstitial fluid flow along white matter tracts: a potentially important mechanism for the dissemination of primary brain tumors. *J. Neuroonc*. **32**, 193.

Giese A, Westphal M (1996) Glioma invasion in the central nervous system. *Neurosurg*. **39**, 235.

Giese A, Loo MA, Rief MD, Tran N, Berens ME (1995) Substrates for astrocytoma invasion. *Neurosurg*. **37**, 294.

Giese A, Loo MA, Tran N, Haskett D, Coons SW, Berens ME (1996) Dichotomy of astrocytoma migration and proliferation. *Int. J. Cancer* **67**, 275.

Haji-Karim M, Carlsson J (1978) Proliferation and viability in cellular spheroids of human origin. *Cancer Res*. **38**, 1457.

Helmlinger G, Netti PA, Lichtenbeld HC, Melder RJ, Jain RK (1997) Solid stress inhibits the growth of multicellular tumor spheroids. *Nat. Biotechnol*. **15**, 778.

Hoshino T, Wilson CB (1975) Review of basic concepts of cell kinetics as applied to brain tumors. *J. Neurosurg*. **42**, 123.

Kleinman HK, McGarvey ML, Hassell JR *et al.* (1986) Basement membrane complexes with biological activity. *Biochem*. **25**, 312.

Koochekpour S, Jeffers M, Rulong S *et al.* (1997) Met and hepatocyte growth factor/scatter factor expression in human gliomas. *Cancer Res*. **57**, 5391.

Kraus M, Wolf B (1993) Emergence of self-organization in tumor cells: relevance for diagnosis and therapy. *Tumor Biol*. **14**, 338.

Landry J, Freyer JP, Sutherland RM (1981) Shedding of mitotic cells from the surface of multicell spheroids during growth. *J. Cell. Physiol*. **106**, 23.

Lang FF, Miller DC, Koslow M, Newcomb EW (1994) Pathways leading to glioblastoma multiforme: a molecular analysis of genetic alterations in 65 astrocytic tumors. *J. Neurosurg*. **81**, 427.

Leon SP, Zhu J, Black PM (1994) Genetic aberrations in human brain tumors. *Neurosurg*. **34**, 708.

Lois C, Garcia-Verdugo J-M, Alvarez-Buylla A (1996) Chain migration of neural precursors. *Science* **271**, 978.

Louis DN (1997) A molecular genetic model of astrocytoma histopathology. *Brain Pathol*. **7**, 755.

Lund-Johansen M, Forsberg K, Bjerkvig R, Laerum OD (1992) Effects of growth factors on a human glioma cell line during invasion into rat brain aggregates in culture. *Acta Neuropathol*. **84**, 190.

Marusic M, Bajzer Z, Freyer JP, Vuk-Pavlovic S (1994) Analysis of growth of multicellular tumour spheroids by mathematical models. *Cell Prolif*. **27**, 73.

Nazarro JM, Neuwelt EA (1990) The role of surgery in the management of supratentorial intermediate and high-grade astrocytomas in adults. *J. Neurosurg*. **73**, 331.

Nishikawa R, Ji X-D, Harmon RC *et al.* (1994) A mutant epidermal growth factor receptor common in human glioma confers enhanced tumorigenicity. *Proc. Natl. Acad. Sci. USA* **91**, 7727.

Nygaard SJT, Pedersen P-H, Mikkelsen T, Terzis AJA, Tysnes O-B, Bjerkvig R (1995) Glioma cell invasion visualized by scanning confocal laser microscopy in an in vitro co-culture system. *Invasion Metastasis* **15**, 179.

Parish CR, Jakobsen KB, Coombe DR (1992) A basement-membrane permeability assay which correlates with the metastatic potential of tumour cells. *Int. J. Cancer* **52**, 378.

Pedersen P-H, Marienhagen K, Mork S, Bjerkvig R (1993) Migratory pattern of fetal rat brain cells and human glioma cells in the adult rat brain. *Cancer Res*. **53**, 5158.

Repesh LA (1989) A new in vitro assay for quantitating tumor cell invasion. *Invasion Metastasis* **9**, 192.

Schwab ED, Pienta KJ (1996) Cancer as a complex adaptive system. *Med. Hypotheses* **47**, 235.

Silbergeld DL, Chicoine MR (1997) Isolation and characterization of human malignant glioma cells from histologically normal brain. *J. Neurosurg*. **86**, 525.

Straeuli P, In-Albon A, Haemmerli G (1983) Morphological studies on V2 carcinoma invasion and tumor-associated connective tissue changes in the rabbit mesentery. *Cancer Res*. **43**, 5403.

Suh O, Weiss L (1984) The development of a technique for the morphometric analysis of invasion in cancer. *J. theor. Biol*. **107**, 547.

Sutherland RM (1988) Cell and environment interactions in tumor microregions: the multicell spheroid model. *Science* **240**, 177.

Sutherland RM, McCredie JA, Inch WR (1971) Growth of multicell spheroids in tissue culture as a model of nodular carcinomas. *J. Natl. Cancer Inst*. **46**, 113.

Tamaki M, McDonald W, Amberger VR, Moore E, Del Maestro RF (1997) Implantation of C6 astrocytoma spheroid into collagen type I gels: invasive, proliferative, and enzymatic characterizations. *J. Neurosurg*. **87**, 602.

Turner GA, Weiss L (1980) Some effects of products from necrotic regions of tumours on the in vitro migration of cancer and peritoneal exudate cells. *Int. J. Cancer* **26**, 247.

Wakimoto H, Aoyagi M, Nakayama T *et al.* (1996) Prognostic significance of Ki-67 labeling indices obtained using MIB-1 monoclonal antibody in patients with supratentorial astrocytomas. *Cancer* **77**, 373.

Whittle IR (1996) Management of primary malignant brain tumors. *J. Neurol. Neurosurg. Psychiatry* **60**, 2.

Yuhas JM, Li AP, Martinez AO, Ladman AJ (1977) A simplified method for production and growth of multicellular tumor spheroids. *Cancer Res*. **37**, 3639.